JGR Oceans

RESEARCH ARTICLE
10.1029/2022JC018724

Multidecadal Water Mass Dynamics on the West Greenland Shelf

J. Mortensen[1], S. Rysgaard[1,2,3], M. H. S. Winding[1], T. Juul-Pedersen[1], K. E. Arendt[4], H. Lund[5], A. E. Stuart-Lee[6], and L. Meire[1,6]

[1]Greenland Climate Research Centre, Greenland Institute of Natural Resources, Nuuk, Greenland, [2]CHR Faculty of Environment Earth and Resources, Centre for Earth Observation Science, University of Manitoba, Winnipeg, MB, Canada, [3]Department of Biology, Arctic Research Centre, Aarhus University, Aarhus, Denmark, [4]SCIENCE, Research and Innovation, University of Copenhagen, Frederiksberg, Denmark, [5]Greenland Institute of Natural Resources, Nuuk, Greenland, [6]Department of Estuarine and Delta Systems, NIOZ Royal Netherlands Institute of Sea Research, Yerseke, The Netherlands

Abstract The waters on the West Greenland continental shelf and slope play an important role in the global climate system with their link to the subpolar North Atlantic Ocean circulation system and the Greenland Ice Sheet. Lately, low temperature waters on the West Greenland shelf have been observed as far south as ~64°N and associated with a cold and relatively saline water mass originating north of Davis Strait in Baffin Bay referred to as Baffin Bay Polar Water (BBPW). Here we use long, seasonal hydrographic time series from West Greenland at ~64°N to study how frequently BBPW is reaching this far south. The analysis covers the period 1950–2018 with a data gap between 1988 and 2005. BBPW was observed frequently and was responsible for the temperature changes observed in the late 1960s–1980s and more intermittently post-2008. Some of the large temperature changes we observe in the time series have previously been ascribed to "Great Salinity Anomalies" (GSAs) propagating around the subpolar North Atlantic Ocean circulation system. The prevailing view of the propagation of GSAs has been ascribed to advection of anomalies along the large-scale circulation system. Our study shows that BBPW may play an important role in the interpretation of GSAs and melt of the Greenland Ice Sheet. Large temporal temperature changes at ~64°N are associated with arrival of BBPW from the north and not advection of anomalies with the large-scale current system from the south. This advocates for a shift in water masses caused by changes in the position and/or strength of oceanic currents.

Plain Language Summary The Greenland Ice Sheet is likely to experience significant mass losses in coming decades. One of the challenges is to understand the changing physical nature of waters on the adjacent continental shelf and their effects on tidewater glacier fjords. Lately, low temperature waters on the West Greenland shelf have been observed as far south as ~64°N and associated with a cold and relatively saline water known as Baffin Bay Polar Water (BBPW) mass originating north of Davis Strait in Baffin Bay. We use unique, long, seasonal hydrographic time series from the West Greenland continental shelf at ~64°N and an adjacent proglacial fjord to study how frequently BBPW is reaching this far south in the period 1953–2018. BBPW was observed at ~64°N in the following years: 1954–1955, 1968–1976, 1980–1983, 1985, 1987, 2008, 2012, and 2015–2017. This study shows that BBPW may play an important role in the interpretation of the large-scale subpolar North Atlantic Ocean circulation system and melt of the Greenland Ice Sheet.

Key Points:

- We present long-term seasonal hydrographic time series from the West Greenland shelf at 64°N and adjacent proglacial fjord
- The time series reveal the recurrence of Baffin Bay Polar Water (BBPW), a northern water mass originating in Baffin Bay
- Large temporal temperature changes are associated with arrival of BBPW and not advection of anomalies with the large-scale current system

Supporting Information:

Supporting Information may be found in the online version of this article.

Correspondence to:

J. Mortensen,
jomo@natur.gl

Citation:

Mortensen, J., Rysgaard, S., Winding, M. H. S., Juul-Pedersen, T., Arendt, K. E., Lund, H., et al. (2022). Multidecadal water mass dynamics on the west Greenland shelf. *Journal of Geophysical Research: Oceans*, *127*, e2022JC018724. https://doi.org/10.1029/2022JC018724

Received 6 APR 2022
Accepted 15 JUN 2022

1. Introduction

Low temperature waters of Baffin Bay origin have lately been observed as far south as ~64°N on the West Greenland continental shelf and slope by Rysgaard et al. (2020). This cold and relatively saline water mass has its origin north of Davis Strait in Baffin Bay, Figure 1a and is here referred to as Baffin Bay Polar Water (BBPW). According to Rysgaard et al. (2020), who yield a detailed description of the water mass and its distribution on the West Greenland shelf, BBPW is a *winter mode water* that is, formed by winter convection north of Davis Strait. In the literature, BBPW has been classified as or referred to as Polar Water, Polar Surface Water, Arctic Water, Baffin Bay Arctic Water, West Greenland Current Polar Water, Arctic Basin Polar Water, or winter Atlantic Water (Addison, 1987; Bourke et al., 1989; Buch et al., 2004; Curry et al., 2011; Gladish et al., 2015; Muench, 1970; Myers et al., 2009; Randelhoff et al., 2019). In a temperature-salinity (*T*-*S*) diagram, BBPW is described by a single point due to the uniform properties obtained during the convection processes (Figure 2). Due to subsequent

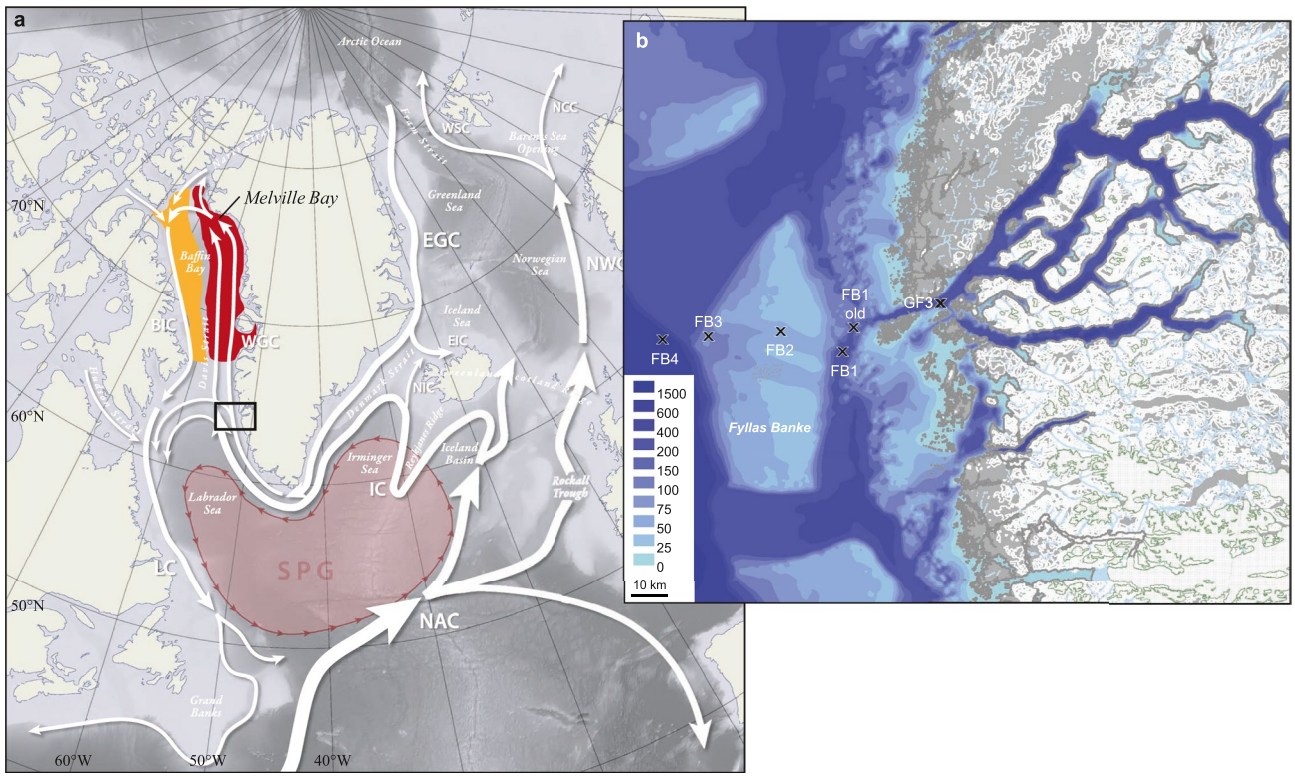

Figure 1. (a) Schematic outline of the distribution of Baffin Bay Polar Water (BBPW) in Baffin Bay. Red is for the BBPW layer found close to the surface and yellow for the BBPW layer found at a deeper level. Also shown are a generally accepted schematic representation of the upper ocean currents making up the subpolar North Atlantic Ocean circulation system. Black box the research area shown in (b) BIC, Baffin Island Current; EGC, East Greenland Current; EIC, Eastern Icelandic Current; IC, Irminger Current; LC, Labrador Current; NAC, North Atlantic Current; NCC, North Cape Current; NIC, North Icelandic Irminger Current; NWC, Norwegian Current; WGC, West Greenland Current; WSC, West Spitsbergen Current. The outline of the subpolar gyre (SPG) is shown in light red. Gray shading denotes bathymetry (the basis Figure is adapted from Tesdal & Haine, 2020, Figure 1, JGR-Oceans). (b) Map of the Nuup Kangerlua system and the adjacent continental shelf and slope, showing locations of hydrographic stations as crosses.

advection by the flow field, BBPW is observed as a "knee" in *T*-*S* space that is, a characteristic inflection close to a salinity of 33.6 and a temperature close to the freezing point (~−1.8°C).

BBPW is found over large parts of Baffin Bay (Figure 1a), occurring in a layer close to the surface in the eastern part near Greenland (e.g., Addison, 1987; Bâcle et al., 2002; Burgers et al., 2017; Mortensen, 2015; Randelhoff et al., 2019; Rysgaard et al., 2020), and in a layer located much deeper and below another water mass (in Davis Strait referred to as e.g., Arctic Water or Baffin Bay Arctic Water) in the western part close to Baffin Island (e.g., Bâcle et al., 2002; Burgers et al., 2017; Gladish et al., 2015; Lehmann et al., 2022; Randelhoff et al., 2019). The formation site of BBPW is still not known in detail. A schematic view of the formation process associated with a "knee" water in *T*-*S* space have been presented by Kikuchi et al. (2004) for the eastern Arctic Ocean. In Baffin Bay, it may be linked to the North Water Polynya (e.g., Addison, 1987; Bâcle et al., 2002; Burgers et al., 2017; Melling et al., 2001) and the eastern part of Baffin Bay in connection with the West Greenland shelf. The formation of BBPW has been observed and visualized in a few cases in connection with North Water Polynya studies close to Greenland between 76°N and 78°N in April 1998 by Melling et al. (2001) and Bâcle et al. (2002). There is presently no observational evidence of BBPW formation on the eastern side of Baffin Bay from Melville Bay and southward down to Davis Strait.

The distribution of water masses is generally set by the circulation system. The West Greenland shelf and slope is part of a large-scale circulation system referred to as the subpolar North Atlantic Ocean circulation system, where the subpolar Gyre (SPG) is a subsystem close to West Greenland (e.g., Tesdal & Haine, 2020). A generally accepted description of the subpolar North Atlantic Ocean circulation system was provided more than a century ago (Figure 1a; e.g., Nansen, 1912; Wüst, 1928). The general circulation in West Greenland is characterized by the northward flowing West Greenland Current (WGC) with no sign of a southward coastal transport. However,

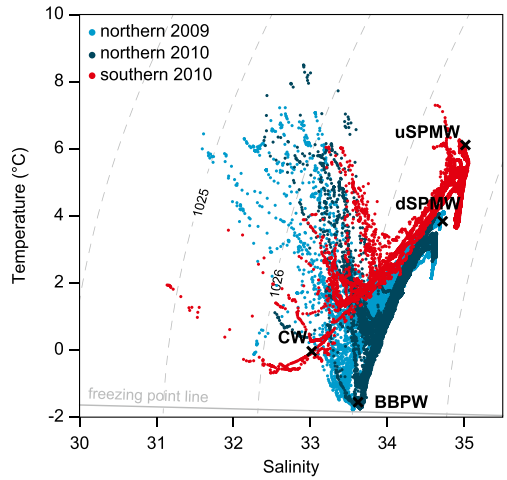

Figure 2. Temperature-salinity (*TS*) plots for west Greenland waters during early summer 2009 and 2010. The 2010 data have been divided into northern (dark blue points) and southern (red points) parts, whereas only northern (light blue points) data are shown for 2009. For north-south division in the northern part of Davis Strait see Rysgaard et al. (2020). Location of water masses are indicated by crosses (x). Upper Subpolar Mode Water (uSPMW), deep Subpolar Mode Water (dSPMW), Baffin Bay Polar Water (BBPW), and Southwest Greenland Coastal Water (CW). Thin gray line indicates the freezing point line at the surface (0 m), and thin broken gray lines indicate isopycnals (adapted from Rysgaard et al. (2020), Figure 5, JGR-Oceans).

Rysgaard et al. (2020) challenge this view, linking a southward transport of BBPW on the West Greenland shelf to the shallow bank systems north of 64°N, which can act as a conveyor belt bringing BBPW southward. This observation is supported by a modeling study by Ribergaard et al. (2004) showing a southward coastal circulation in connection with shelf banks. Ribergaard et al. finds that residual anticyclonic eddies are generated around West Greenland shelf banks. They argue that eddies are consistently observed, and formed from interaction between topography and tides. In a recent modeling and observational study, Myers et al. (2021) described a net transport reversal at the end of 2010 through Davis Strait, which led to a significant northward oceanic heat transport into Baffin Bay. Myers et al. linked the reversal to anomalous winter winds along West Greenland, allowing water of Atlantic origin to propagate northwards into Baffin Bay instead of entering the interior Labrador Sea. The presence of BBPW in West Greenland plays an important role for the melting of the Greenland Ice Sheet. BBPW is one of two water masses found at the coast adjacent to many tidewater glacier fjords in this region (e.g., Bendtsen et al., 2021; Mortensen et al., 2020; Rysgaard et al., 2020). Recent warning and cooling of ocean water in Disko Bay described by Myers and Ribergaard (2013) and Khazendar et al. (2019), respectively, might even be associated with changes in the production and distribution of BBPW.

Some of the large temporal hydrographic changes in West Greenland (observed from long-term hydrographic time series on the continental shelf and slope at ~64°N) have previously been ascribed to "Great Salinity Anomalies" (GSAs) observed in the upper layers of the North Atlantic. Three GSAs propagating around the subpolar North Atlantic Ocean circulation system with timescales of 6–13 years have been reported, occurring in West Greenland in 1969–1970, 1982, and 1989–1990 (Belkin, 2004; Belkin et al., 1998; Dickson et al., 1988). The GSA'70 was apparently formed by enhanced Arctic Ocean freshwater export via Fram Strait, whereas the GSA'80 and GSA'90 were formed locally in the Labrador Sea/Baffin Bay area. The propagation of GSAs has been ascribed to advection of property anomalies along the large-scale circulation system (e.g., Belkin et al., 1998; Dickson et al., 1988). However, an *alternative* hypothesis proposed that changes are horizontal *shifts of water masses* such as shifts in the Sub-Arctic Front west of Britain (Dooley et al., 1984; Ellett & MacDougall, 1983; Martin et al., 1984). However, these shifts were only observed in connection with the Subpolar Gyre south of Iceland and have lately attracted renewed focus (e.g., Hátún et al., 2016; Holliday et al., 2020; Kenigson & Timmermans, 2021).

A growing number of coupled climate models have been used to explore climate models' ability to produce GSAs (e.g., Bigg & Wadley, 2007; Haak et al., 2003; Kim et al., 2021; Wadley & Bigg, 2004). Where most models support the advection hypothesis, model work by Wadley and Bigg (2006), however, questions the advection hypothesis. Wadley and Bigg (2006) concludes that GSAs are unlikely to be caused by the advection of salinity anomalies, but rather anomalous oceanic currents or surface fluxes are responsible. A tracer release in their model suggests that horizontal advection of the tracer in the upper ocean is limited to around 1,000 km. Rysgaard et al. (2020) used BBPW to challenge the generally accepted description of the subpolar North Atlantic Ocean circulation system by introducing a southward flowing current in connection with the West Greenland shelf. We use BBPW to challenge the generally accepted view of GSAs and their advection of property anomalies around the subpolar North Atlantic Ocean circulation system.

In this paper, we present long hydrographic time series (1950–2016) from the Fyllas Banke section at 64°N, West Greenland, as well as a nearby long, seasonal time series from the outer sill region of the proglacial fjord system Nuup Kangerlua (Godthåbsfjord). Our analysis focuses on how frequently BBPW is reaching this far south on the West Greenland coast. We explore the link between BBPW and GSAs, that is, the large-scale regional circulation system of the subpolar North Atlantic Ocean.

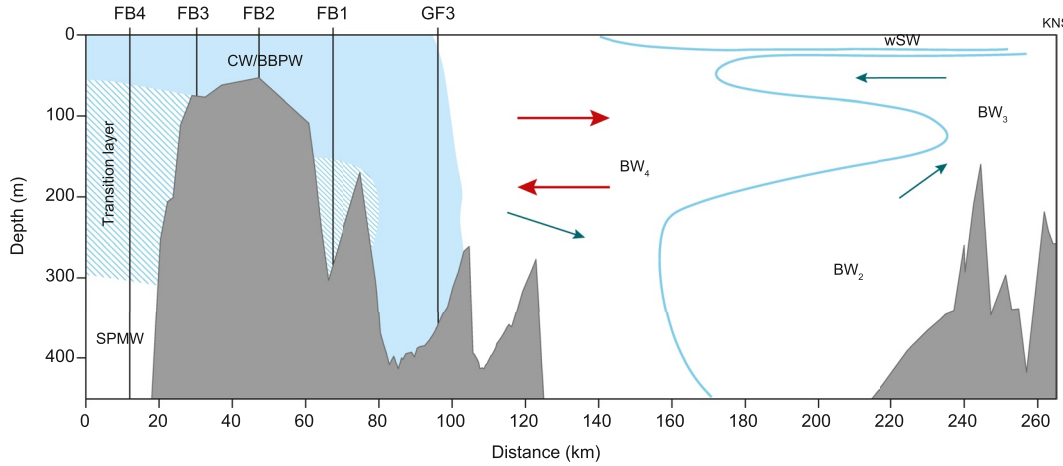

Figure 3. Schematic representation of present knowledge of the circulation system and distribution of water masses in Nuup Kangerlua during late winter (based on Mortensen et al., 2011, 2013, 2014, 2018). BBPW: Baffin Bay polar water; CW: Southwest Greenland coastal water; SPMW: subpolar mode water; wSW: winter surface water; BW_i: basin water types $i = 2–4$; KNS: Kangiata Nunaata Sermia. Dense coastal inflow, blue arrows; and intermediate baroclinic circulation, red arrows. Vertical lines indicate the location of the different hydrographic station used in the text. Fjord water masses are discussed in Mortensen et al. (2018) (the basic figure is adapted from Mortensen et al., 2018, Figure 2b, JGR-Oceans).

2. Study Area and Methodology

2.1. Settings and Water Masses

Fyllas Banke and Nuup Kangerlua are located on the West Greenland coast (~64°N). Fyllas Banke is a shallow bank on the continental shelf with minimum depths less than ~40 m found adjacent to Nuup Kangerlua (Figures 1b and 3). Nuup Kangerlua is one of the largest proglacial fjord systems in Greenland, covering a surface area of 2,013 km^2 (Mortensen et al., 2011, 2018). The main fjord branch is 190 km long and the connection to Fyllas Banke is restricted by a ~200 m deep entrance sill. The fjord system is characterized by M_2 tidal amplitudes above 1 m and a tidal range between 3 and 5 m (Padman et al., 2018; Richter et al., 2011).

Below we make use of a water mass classification introduced for West Greenland and discussed in detail by Rysgaard et al. (2020). The classification is the first of its kind to distinguish between the two cold and fresh water masses found on the West Greenland shelf. It is based on the classification by McCartney and Talley (1982), Mortensen et al. (2011, 2018) and the Greenland Institute of Natural Resources' standard hydrographic coastal monitoring program (Mortensen, 2015). The coastal waters at Fyllas Banke are characterized by three distinct water masses: Southwest Greenland Coastal Water (CW), BBPW and Subpolar Mode Water (SPMW), where BBPW and SPMW are winter mode water masses. The upper layer is composed of a northward flow of relatively cool and fresh CW, the southern freshwater source (*T-S* properties ~0 °C and 33.0), which originates in the East Greenland Current and is modified by surface fluxes and runoff from Greenland. The upper layer is intermittently occupied by the presence of a southward flow of cold and relatively saline BBPW (*T-S* properties ~−1.8 °C and 33.6), with an origin in Baffin Bay north of Davis Strait. In the layer below, a northward flow of warmer and more saline SPMW of Atlantic origin is present. This water mass is further divided into upper SPMW (uSPMW, *T-S* properties ~6 °C and 35) and deep SPMW (dSPMW, *T-S* properties ~4 °C and 34.9) layers. Rysgaard et al. (2020) recently discussed the distribution of water masses along the west coast of Greenland from Cape Farwell (59°N) to Kullorsuaq (75°N).

A schematic representation of the distribution of water masses on Fyllas Banke and in Nuup Kangerlua during late winter is summarized in Figure 3 (based on Mortensen et al. (2011, 2013, 2014, 2018)). During late winter, coastal water masses are observed at the outer sill region including the standard hydrographic station GF3 described below (Mortensen et al., 2011, 2018). During summer, the outer sill region is mainly occupied by fjord water masses (Mortensen et al., 2011, 2018). Overlaid on Figure 3 is the winter circulation system for the fjord characterized by two different circulation modes: dense coastal inflows and intermediate baroclinic circulation. Dense coastal inflow driven by coast-fjord density gradients are observed during the winter months in the deeper

parts of the fjord. The intermediate baroclinic circulation is driven by tidal-induced diapycnal mixing in the outer sill region (Mortensen et al., 2011, 2014). This mixing leads to a horizontal density gradient between the outer sill region and the main fjord and drives the intermediate baroclinic circulation (Figure 3).

2.2. Data

The data set used in this study consists of data from four long hydrographic time series from the Fyllas Banke section located on the West Greenland continental shelf and collected by the Greenland standard hydrographic coastal monitoring program operated by the Greenland Institute of Natural Resources (Figure 1b). Hydrographic stations found within a search radius of 3 km from the standard positions were used for this study (FB1: 64°01′N, 52°19′W, depth ∼108 m, and post 1986 63°57′N, 52°22′W, depth ∼273 m; FB2: 63°58′N, 52°44′W, depth ∼47 m; FB3: 63°55′N, 53°07′W, depth ∼72 m; FB4: 63°53′N, 53°22′W, depth ∼956 m). Fyllas Banke data were obtained for the period between 1950 and 2016. The sampling frequency of the Fyllas Banke stations varied from seasonal occupations (usually 5–6 annual cruises) in the period 1968 to 1988, to 1–3 annual cruises in the periods: 1950–1967 and 1989–2016, see Figure S1 in Supporting Information S1. Hydrographic data for the Fyllas Banke analysis were identified using CTD and bottle measurements from the International Council for the Exploration of the Sea (ICES) Oceanography Data Portal (http://www.ices.dk) and May data in the period 2006–2016 from the Greenland Ecosystem Monitoring Program (www.g-e-m.dk). Practical salinity scale (PSU) is used throughout the text.

Data from the hydrographic standard station GF3 (64°07′N, 51°53′W, depth ∼350 m) in the outer sill region of Nuup Kangerlua (Juul-Pedersen et al., 2015; Mortensen et al., 2018) comprise a fifth time series (Figure 1b). Hydrographic data for the GF3 analysis were identified by CTD and bottle measurements from the ICES Oceanography Data Portal (http://www.ices.dk) during the period 1953–1988. Hydrographic data during the later period 2005–2018 were obtained from the Greenland Ecosystem Monitoring Program (www.g-e-m.dk). The sampling frequency for GF3 is close to monthly during two periods: 1954–1968 and 2005–2018, with 6–7 annual cruises in the period 1969–1985, see Figure S1 in Supporting Information S1. Note that a relatively large number of salinity values were lost during the first period (1953–1988), Figure S1 in Supporting Information S1. This is especially prominent for 1979 where all salinity water samples were lost, likely damaged or lost during transport to Copenhagen, Denmark, where salinity determination took place.

3. Results and Discussion

3.1. Variability in the Outer Fjord (GF3)

Depth-time contour plots of temperature and salinity at the outer fjord site GF3 for the periods 1953–1988 and 2005–2018 are presented in Figure 4. These plots show considerable seasonal and interannual variation in both parameters at all depths. Property ranges for the two periods were ($-1.5°C \leq T \leq 7.93°C$; $22.49 \leq S \leq 34.56$) and ($-1.04°C \leq T \leq 8.48°C$; $18.48 \leq S \leq 34.37$), respectively, with limits for the latter period being warmer and fresher. In addition to the contour plots, time series of temperature and salinity at the outer fjord station at three selected depths: 50, 150, and 240 m, are shown in Figure 5.

Considering the first period (1953–1988), a warm period was observed between 1953 and 1967 with seasonal temperature frequently found above 2°C, Figures 4a and 4ure 5. During this warm period 1953–1967, the water column experienced temperatures in the range 0–4°C with the highest temperatures in the range 3–4°C occurring at the ends of 1960 and 1961. Furthermore, winter temperatures were seldom below 0°C (Figure 5). This warm period was followed by two cold periods, 1968–1976 and 1980–1982, where the water column seldom reached temperatures above 2 °C and during which winter temperatures were well below 0 °C. The salinity time series (Figures 4b and 5) reveals a relatively saline period between 1953 and 1961 with seasonal salinities frequently found above 33.5 at depth. This period was followed by a gradual freshening of the water column in the period 1962–1970, as seen in Figure 5, and as a deepening of the 33.5 isohaline in Figure 4b. Prior to the cooling in 1980, a relatively fresh water column was observed in the period 1976–1980 with seasonal salinities found below 33.5.

The second period (2005–2018) in Figure 4a was characterized by an extreme warm period between 2010 and 2011, with temperatures frequently found above 3°C. The extreme warm period was found between two warm periods: 2005–2009 and 2012–2018, with temperatures frequently found above 2 °C and a few cold winters

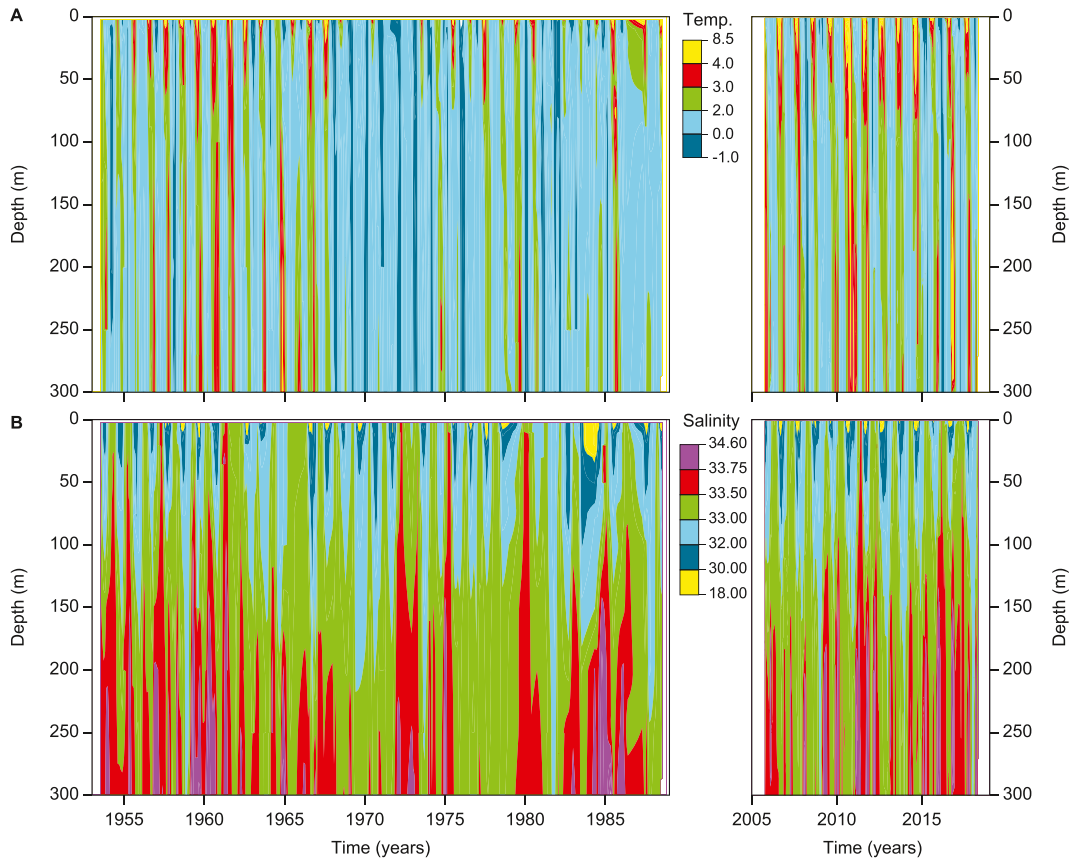

Figure 4. Depth-time contour plots of (a) temperature and (b) salinity for the outer fjord station GF3 for the periods 1953–1988 and 2005–2018.

(i.e., $T < 0$ °C) in 2008, 2015, 2016, and 2017. The warmest water arrived at the end of summer 2010, when the highest temperatures (>4 °C) associated with a locally formed coastal water mass entered the fjord (Mortensen et al., 2018).

To summarize, Figures 4a and 5 show that comparable seasonal temperature structures were observed in the first (1953–1967) and last (2005–2018) periods, characterized by seasonal temperatures in the range of 0–4 °C. Low temperatures were found in two intermediate periods, 1968–1976 and 1980–1982, characterized by seasonal temperatures in the range of −1 to 2 °C. The overall temperature maximum for the entire period (1953–2018) occurred in 2010, followed by a continuous temperature decrease lasting until at least 2018. The long-term salinity structure was described by comparably high salinities in the first (1953–1962) and last (2014–2018) periods, characterized by seasonal salinities frequently above 33.5. Low salinities were found in two intermediate periods, 1963–1972 and 1976–1979, characterized by seasonal salinities frequently found below 33.5, Figures 4b and 5.

Cold periods observed at the coast, discussed below, have in the past been associated with GSAs passing Fyllas Banke (Belkin et al., 1998; Dickson et al., 1988). The cold periods in the outer fjord according to Figure 5 arrived in 1968 and 1980 at all depths, that is, 1–2 years ahead of the previously estimated times for the coast in 1969–1970 and 1982. In the fjord, these cold periods or events are observed as a sudden shift in temperature and linked to the arrival of cold winter water (i.e., with temperatures below 0 °C) compared to the winter before (Figure 5). Both cold periods 1968–1976 and 1980–1982 were characterized by cold winter water with temperature well below 0 °C. The 3 years mean salinity in Figure 5 suggests a minor increase in connection with cold period arrivals in 1968 and 1980, yet the pattern is not that clear. The arrival of the short warm period in 2010 was observed as a sudden shift in the later summer temperature (i.e., an increase in temperature) with an associated decrease in salinity (Mortensen et al., 2018).

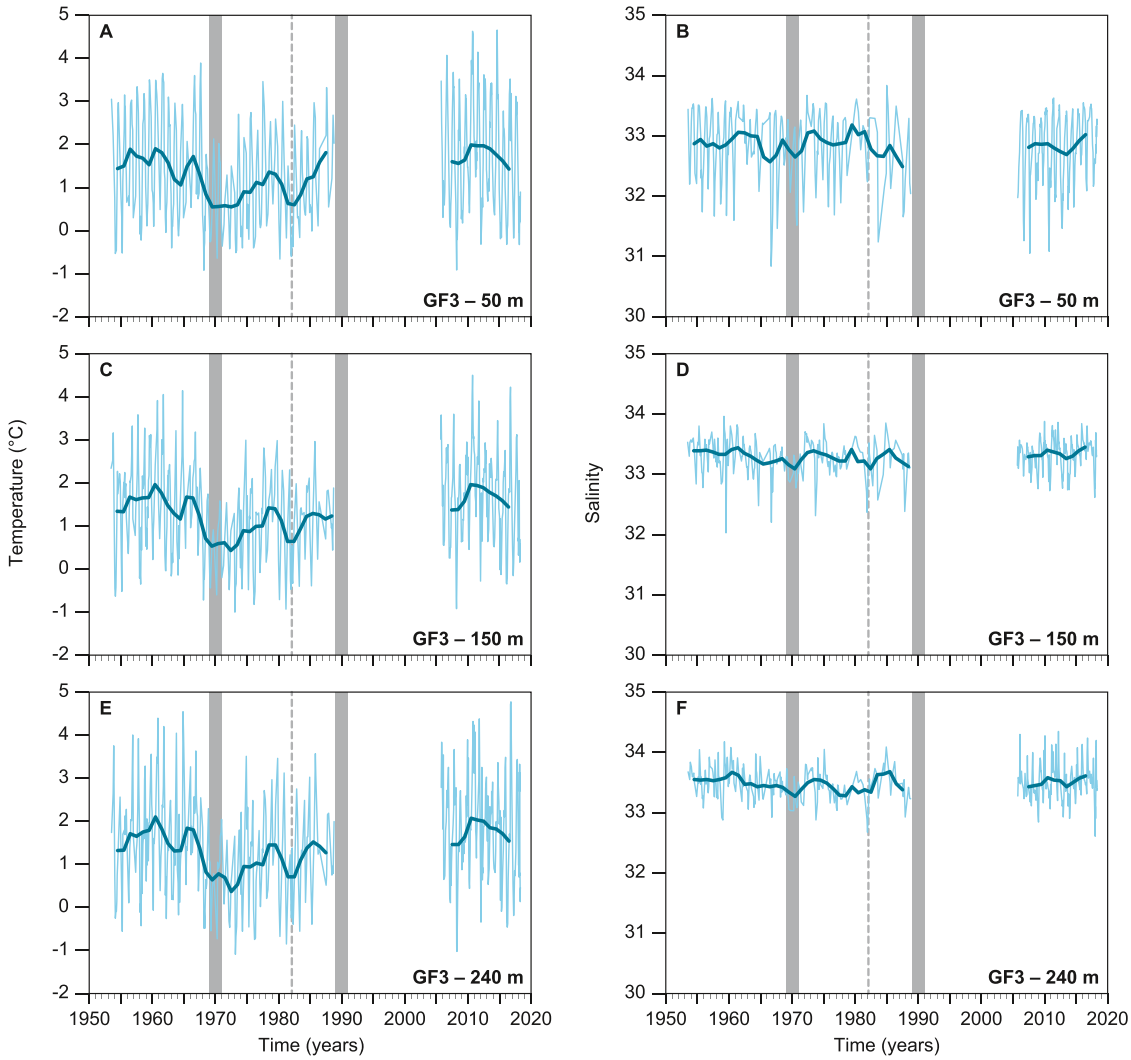

Figure 5. Time series of temperature and salinity for the outer fjord time series (GF3) for three depth levels: (a) and (b) 50 m, (c) and (d) 150 m, and (e) and (f) 240 m, respectively, in the two periods 1953–1988 and 2005–2018, thick line 3 years mean. The arrival times/periods at Fyllas Banke for three Great Salinity Anomalies according to literature are indicated by vertical gray features (1969–1970, 1982, and 1989–1990).

Based on monthly mean property isopleths from 1969 to 1978, the seasonal temperature range at GF3 was ∼3 °C at 50 m depth with minimum values in March-April and maximum in August, Figure 6. With increasing depth, the seasonal temperature signal was less regular, Figure 5. The lowest (−1.09 °C in March 1973) and highest (4.77 °C in October 2016) temperatures at the three depths for the entire period were observed at 240 m. The salinity time series in Figure 5 reveals that there was a seasonal salinity signal at 50 m, with a less distinct signal below. At 50 m the seasonal salinity range was ∼1.5 PSU with maximum values in May-June and minimum in October, Figure 6. At 50 m depth the seasonal signal is mainly linked to the seasonal freshwater runoff to the fjord, whereas this link to runoff was lost with depth as water properties became gradually more influenced by sporadic coastal exchange. The highest recorded salinity of 34.35 was observed in March 2012 at 240 m depth and the lowest of 30.84 was observed in September 1966 at 50 m depth. Figure 6 reveals the importance of seasonal hydrographic monitoring programs for understanding the multidecadal water mass dynamics on the West Greenland shelf.

3.2. Variability at the Fyllas Banke Section (FB1–FB4) and Its Link to the Fjord

In contrast to the high frequency sampling at the outer fjord station GF3, the four standard stations at the Fyllas Banke section (FB1–FB4) were not sampled monthly (Figure S1 in Supporting Information S1). Figure 7

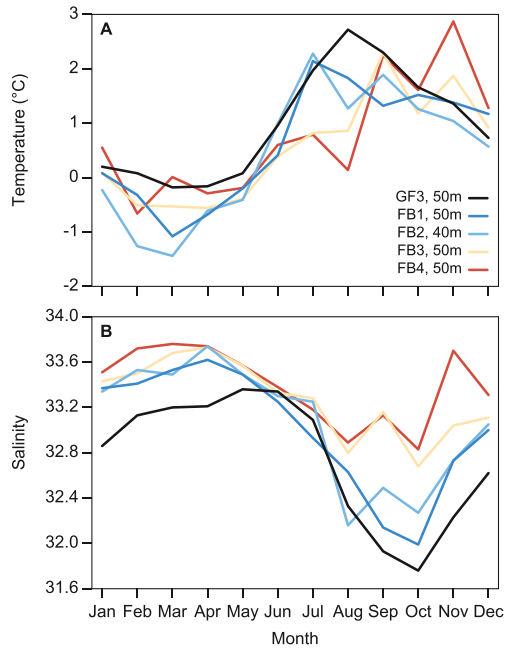

Figure 6. Monthly mean (a) temperature (°C) and (b) salinity isopleths at 50 m depth for the 10 year period from 1969 to 1978 at GF3 (black), FB1 (blue), FB2 (40 m, light blue), FB3 (yellow), and FB4 (red).

shows the time series of temperature and salinity for the four Fyllas Banke stations from 50 m depth and, in the case of FB2, 40 m depth for the period 1950–2016. The plots suggested significant seasonal and interannual variation in both parameters during periods with high sampling rates, Figure S1 in Supporting Information S1. Property ranges at 50 m depth for the four shelf stations FB1–FB4 are shown in Table 1. The coldest and warmest limits were found away from the coast at FB3 and FB4, whereas the freshest water was found close to the coast at FB1. During the two cold periods 1968–1976 and 1980–1982 there is a prior lack of seasonal measurements at all shelf stations FB1–FB4, see Figure S1 in Supporting Information S1. Using GF3 as a baseline (Figure 8) we argue that the two cold periods can be observed at FB1 and FB2 (Figure 7) and, hence, we can effectively build a composite time series for the BBPW water mass discussion below.

Based on monthly mean property isopleths from 1969 to 1978 at 50 m depth on the shelf, the seasonal temperature range was ~3 °C with minimum values in February-March and maximum in July-August/September-November (Figure 6). The maxima occurred later in the outer part of the shelf at FB3 and FB4. During many of the years in the period between 1968 and 1988, the annual temperature minimum was close to the freezing point at FB2 at 40 m depth (Figure 7). Temperatures close to freezing point were observed only in 1973 and 1982 at FB3 and FB4, and not once at FB1. The high number of close-to-freezing-point observations at FB2 might be linked to either the shallowness of the station (~40 m depth), which makes it more exposed to cooling by the atmosphere, or the more frequent presence of BBPW at this station (see below). The highest recorded temperature at the coastal stations in Figure 7 was observed in mid-November 2003 at all stations.

Figure 7 showed that all four shelf stations have an intermittent seasonal salinity signal. Based on monthly mean property isopleths from 1969 to 1978, the seasonal salinity range was ~1–1.5 PSU, with maximum values in February-April and minimum in September-October, and the largest range found close to the coast (Figure 6). The highest recorded salinity was observed in mid-November 2003 at both FB3 and FB4, which is surprising as the autumn is generally characterized by the lowest salinities. The four salinity time series from the shelf reveal that the freshest water was found at the station closest to the coast (FB1), with salinities increasing with distance from the coast. We note that high frequency variability observations in the monthly mean property isopleths in the later part of the year might be artifacts due to the low number of observations during late summer.

The above description of the outer fjord and shelf stations reveals that the near surface waters show similar interannual and seasonal variations. The time series of temperature and salinity for 50 m at FB1 and GF3 for the period 1950–1988 (Figure 8) shows that temporal temperature variation at the coastal station FB1 is to a large degree depicted at the outer fjord time series GF3. The overlaid temperature time series in Figure 8a reveals that the cold events arriving in 1968 and 1980 are well resolved by FB1, when GF3 is used as a baseline. The seasonal minimum temperature observed during winter is generally lower at the coastal station FB1 than at the outer fjord station GF3, Figure 8a. This pattern was observed earlier for a shorter-term comparison between the shelf and outer fjord station (Mortensen et al., 2018).

3.3. BBPW Reaching the Fyllas Banke Section

Figure 9 shows all salinity and temperature records from the shelf (FB1–FB4) and outer fjord (GF3) time series in *TS*-diagrams. These are overlaid with the principal water masses from the coast according to the classification introduced by Rysgaard et al. (2020). Figure 9 reveals that the coldest water mass found at the Fyllas Banke section (FB1–FB4) is associated with BBPW and not CW from the southern freshwater source. At the outer fjord station, GF3, only a warmer version of BBPW is observed, revealed by its relatively high salinity. uSPMW and dSPMW were found over the continental slope at FB4 and not at the shallow bank station FB2. Traces of uSPMW and dSPMW were however observed at FB3 and FB1.

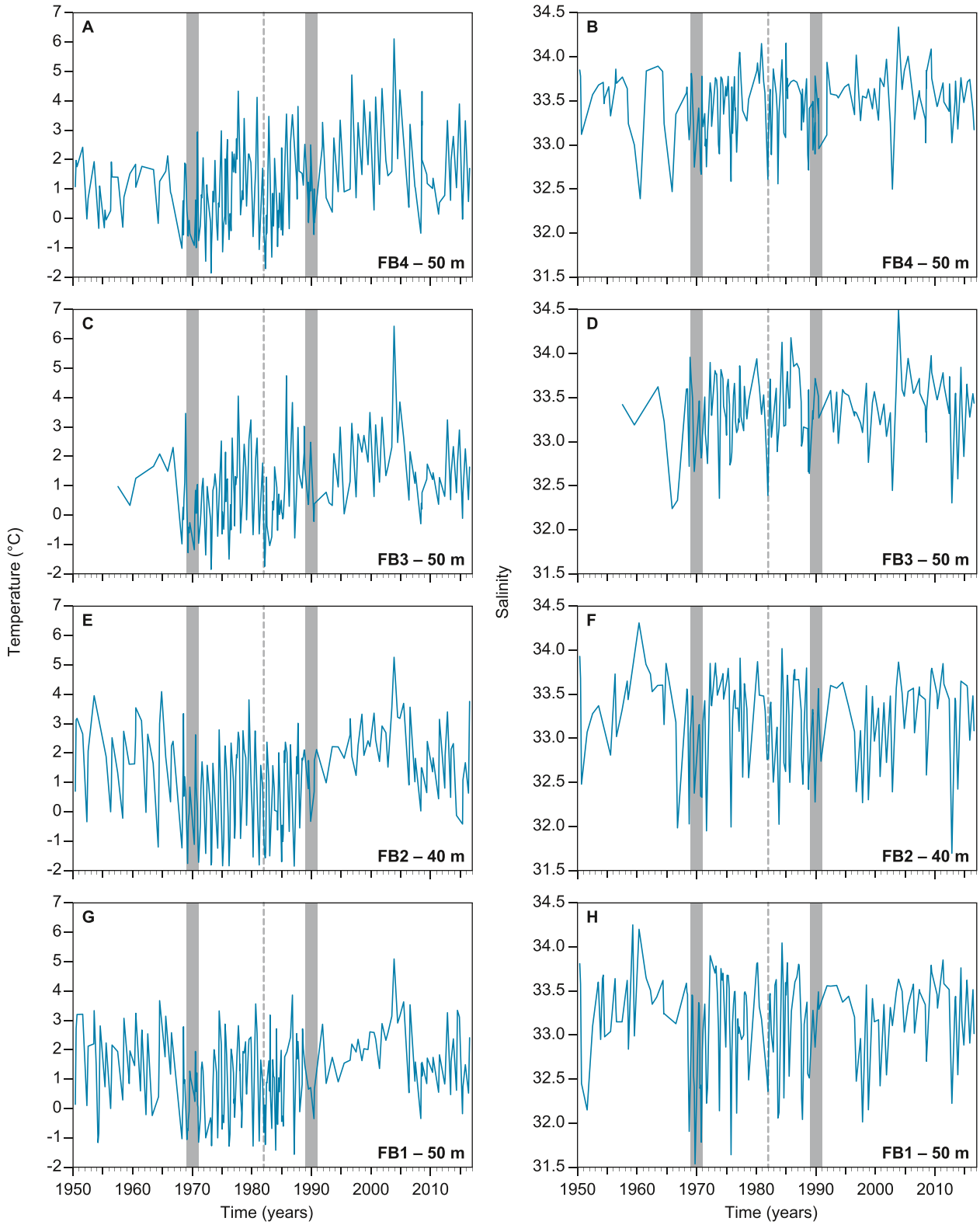

Figure 7. Time series of temperature and salinity at 50 m depth for the four Fyllas Banke stations: (a) and (b) FB4, (c) and (d) FB3, (e) and (f) FB2 (40 m), and (g) and (h) FB1 in the period 1950–2016, respectively. The arrival times/periods at Fyllas Banke for three Great Salinity Anomalies according to literature are indicated by vertical gray features (1969–1970, 1982, and 1989–1990).

Table 1
Temperature and Salinity Conditions at 50 m Depth for Four Shelf Stations (FB1–FB4), in the Case of FB2, 40 m Depth

Station #	Temperature	Salinity
FB1	$-1.56°C \leq T \leq 5.09°C$	$31.54 \leq S \leq 34.25$
FB2	$-1.85°C \leq T \leq 5.26°C$	$31.70 \leq S \leq 34.31$
FB3	$-1.85°C \leq T \leq 6.30°C$	$32.24 \leq S \leq 34.49$
FB4	$-1.86°C \leq T \leq 6.11°C$	$32.39 \leq S \leq 34.33$

Figure 10 shows *TS*-properties for FB2 and the annual June/July mean *TS*-properties (depth averaged between 0 and 40 m) for FB2 in the period 1953–2016. Also shown is the development of the mean *TS*-properties for FB2 for the period March 1969 to August 1969. Where most June/July mean *TS* values are grouped around a limited range in *TS* space (*T*: 0–4 °C and *S*: 33–34) only June 1969 lies outside this grouping. In Dickson et al. (1988), 1969 was interpreted as the year the advective GSA of the 1970s arrived at Fyllas Banke. In the months just before June 1969, the water column at FB2 was occupied by BBPW, with the coldest water found in March and getting progressively warmer through May. In June, BBPW was replaced by CW. From June to August, CW warmed and freshened following the seasonal cycle as depicted in Figure 6. This shows that the observed hydrographic changes in 1969 at FB2 can be explained by a shift in water masses.

The *TS*-diagrams in Figures 9 and 10 indicate that the saline water with temperatures close to the freezing point on the West Greenland continental shelf at FB1–FB4 is most likely associated with BBPW. In the outer fjord (GF3), saline water with temperatures below 0 °C is a good indicator that BBPW is present at the adjacent shelf. Using these indicators, BBPW was observed annually during the two cold periods 1969–1976 and 1980–1983 and in the years: 1985, 1987, and 2008 at the shelf stations (FB1–FB4). The conditions at the outer fjord station (GF3) support the presence of BBPW for most of these years and in addition the following years: 1954–1955, 1968, 2012, and 2015–2017. Merging the data series from the two sites, BBPW was observed at the Fyllas Banke section during the period 1953–2018 in the following years: 1954–1955, 1968–1976, 1980–1983, 1985, 1987, 2008, 2012, 2015–2017. Due to a winter data gap between 1988 and 2005, it is not possible to determine if BBPW was present at Fyllas Bank during those years.

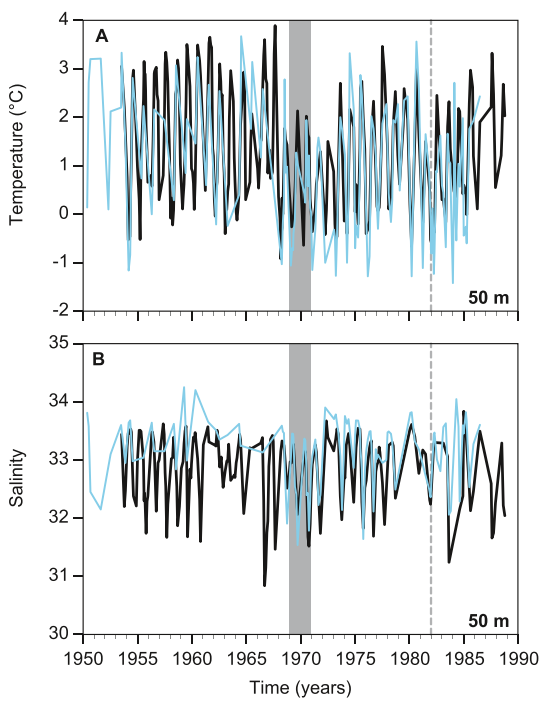

Figure 8. Time series of (a) temperature and (b) salinity for the outer fjord station (GF3, black line) and coastal station (FB1, blue line) at 50 m depth during the period 1950 to 1988. The arrival times/periods at Fyllas Banke for two Great Salinity Anomalies according to literature are indicated by vertical gray features (1969–1970 and 1982).

3.4. Water Mass Dispersion and Link to the Large-Scale Circulation System

The dynamics behind GSAs are questioned by the presence of BBPW on the West Greenland coast at Fyllas Banke, ~64°N. Due to the northern origin of BBPW and timing at Fyllas Banke, GSAs are unlikely to be caused by advection of anomalies that travel along the large-scale regional circulation system, that is, the subpolar North Atlantic Ocean circulation system, Figure 1a. This finding is further supported by model results presented by Wadley and Bigg (2006) who conclude that anomalous oceanic currents or surface fluxes are instead responsible. They based their conclusion on a tracer release in a model, which shows that horizontal advection of the tracer in the upper ocean is limited to around 1,000 km due to mixing and incorporation in the deep water. The changes at West Greenland are more likely local shifts of water masses caused by changes in production of BBPW and in the position and/or strength of oceanic currents. This shows that production of BBPW might be an important factor in understanding the multidecadal water mass changes and their dynamics on the West Greenland shelf. However, winter observations are presently lacking from the West Greenland shelf and the specific BBPW formation site remains largely unknown with one exception suggesting formation at the North Water Polynya close to Greenland between 76°N and 78°N (Bâcle et al., 2002). The huge area covered by BBPW during winters reaching as far south as ~64°N, Figure 11, suggests that the North Water Polynya is not the only formation site. BBPW formation likely takes place on the eastern side of Baffin Bay from Melville Bay in the north and southward down to Davis Strait and even as far south as the Fyllas Banke at 64°N. However, only future winter campaigns can reveal the exact geographic distribution of the BBPW formation in the region.

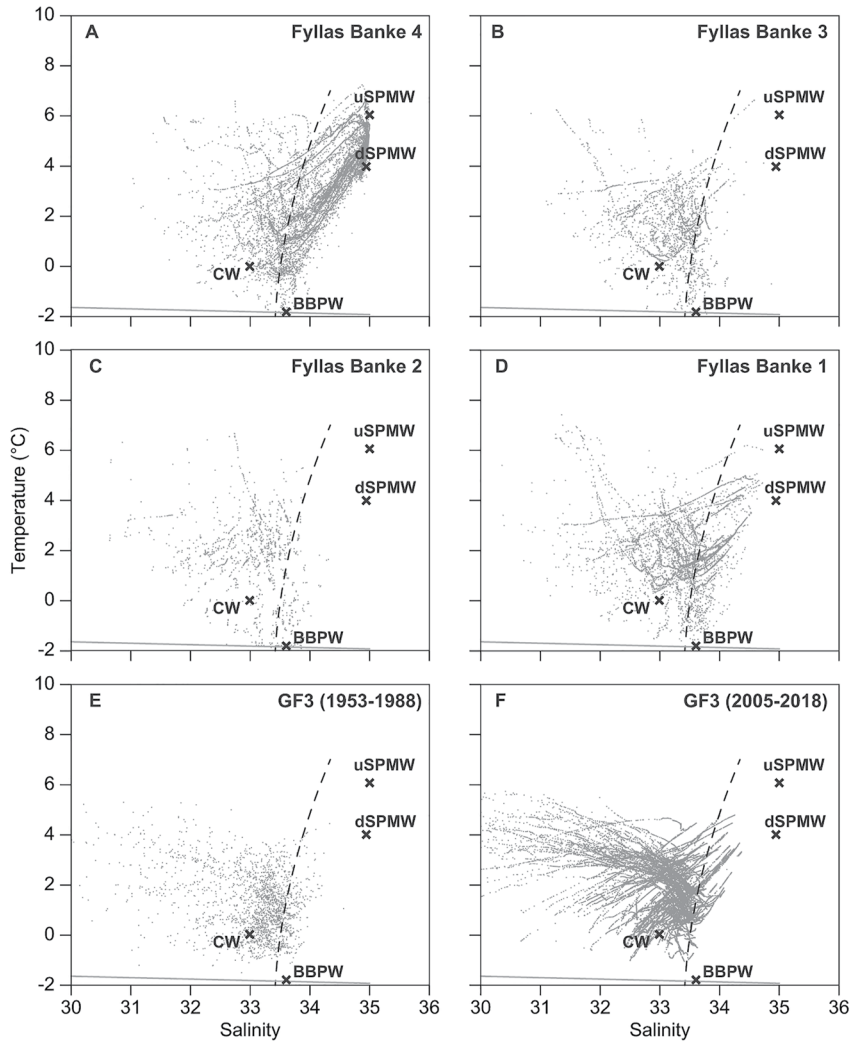

Figure 9. *TS*-diagrams for the four (1950–2016) Fyllas Banke stations (a) FB4, (b) FB3, (c) FB2, (d) FB1, and the outer fjord station (GF3) for the period (e) 1953–1988, and (f) 2005–2018. Locations of water masses are indicated by crosses. Upper subpolar mode water (uSPMW), deep subpolar mode water (dSPMW), Baffin Bay polar water (BBPW), and Southwest Greenland coastal water (CW). Freezing point line is shown as a gray line and the broken gray line indicates the 26.9 isopycnal. Measurements with salinity less than 30 for GF3 are not shown.

BBPW is important for the melt of the Greenland Ice Sheet on the West Greenland coast. Here, BBPW can block the heat input to the fjords in the upper hundreds of meters of water column (Rysgaard et al., 2020). In deep fjords with a shallow entrance sill (≤100 m depth) BBPW may contribute to the deep and bottom waters of the fjord (Stuart-Lee et al., 2021). Further, the years with BBPW at Fyllas Banke have recently been linked with deep convection in the subpolar gyre (SPG), Figure 11, that is, in the Labrador Sea and Irminger Sea (Mortensen et al., 2018).

There is a growing number of studies investigating the atmospheric impact on local oceanic conditions during the period 1950–2020. For example, Myers et al. (2021) used the Greenland Blocking Index and storm track path changes to explain a reversal of the Baffin Bay transport through Davis Strait in winter 2010–2011. The study of Myers et al. (2021) also covers an analysis of the North Atlantic Oscillation (NAO) index and the Arctic Ocean (AO) index. In addition, Liang et al. (2021) investigated long-term data sets covering nearly 40 years of sea ice flux through the Davis Strait and Arctic cyclone activity and show that sea ice concentration and motion fields can be greatly altered by the occurrence of cyclones, thereby contributing to changes in sea ice export. This highlights the need to increase our understanding of the influence of wind conditions on the spatial distribution and variability of sea ice extent and water masses.

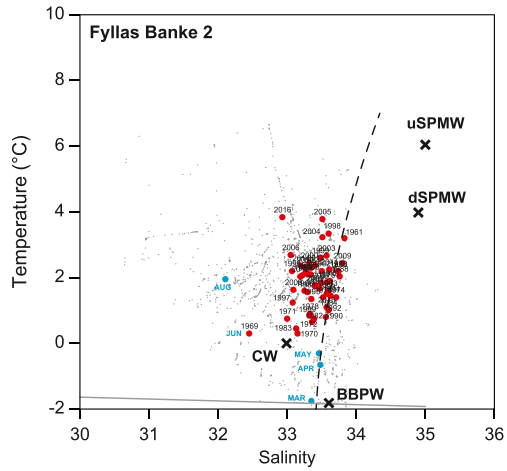

Figure 10. *TS*-diagrams for the Fyllas Banke station FB2, 1950–2016 (gray dots). Red and cyan dots mean *TS* (0–40 m) with measurements in June/July for the period 1950–2016 and seasonal observations in 1969, respectively. Locations of water masses are indicated by crosses. Upper subpolar mode water (uSPMW), deep subpolar mode water (dSPMW), Baffin Bay polar water (BBPW), and Southwest Greenland coastal water (CW). Gray line is the freezing point line and the broken gray line indicates the 26.9 isopycnal.

In summary, BBPW formation and its associated impact on West Greenland waters may be governed by a complex interaction of cyclone occurrences, heat and energy exchange between a cold atmosphere and relatively warm ocean during ice free conditions. Favorable conditions lead to an expansion of the BBPW water mass. In case the BBPW formation site is in the northeastern part of the Baffin Bay, we suggest a southward transport along the West Greenland coast as shown in Figure 11. The southward transport of BBPW on the West Greenland shelf close to the Greenland south Davis Strait has been suggested and linked by Rysgaard et al. (2020) to the shallow bank systems, which can act as a conveyor belt bringing BBPW southward along the coast. We argue here that the same process might take place north of Davis Strait, bringing BBPW southward close to West Greenland, Figure 11. On its way, BBPW blocks CW and SPMW and results in a cooling of West Greenland. This results in a decreased heat transport to fjords and to a reduced oceanic melt at tidewater outlet glaciers. We note that this southward transport of BBPW still remains to be verified by observations. During dominant BBPW conditions, glacier termini are expected to advance in the absence of other processes contributing to their changes. The extreme case in which BBPW is formed along the entire West Greenland coast conforms with the idea of Belkin et al. (1998) that GSA'80 and GSA'90 is formed locally in the Labrador Sea/Baffin Bay.

4. Summary and Conclusions

Long seasonal hydrographic time series from the West Greenland continental shelf at ~64°N and an adjacent proglacial fjord were used to study how frequently the northern water mass BBPW reached this far south during the period 1950–2018. When analyzing data, we used a water mass classification, which can distinguish between the regional southern sources and waters formed to the north in Baffin Bay. Three water masses can be used to explain ~70 years of hydrographic changes (i.e., BBPW, CW, and SPMW). We identified BBPW at the Fyllas Banke section at ~64°N in the following years: 1954–1955, 1968–1976, 1980–1983, 1985, 1987, 2008, 2012, 2015–2017. During these years BBPW was found more than 500 km south of its presumed normal distribution area in the eastern part of Baffin Bay. A winter data gap limited the study of BBPW between 1988 and 2005.

More work is needed to identify the formation site of BBPW, as this water mass is important for blocking CW and SPMW and results in a cooling of West Greenland waters. This results in a decreased heat transport toward fjords and to a reduced oceanic melt at tidewater outlet glaciers. During years with dominant BBPW conditions, glacier termini are expected to advance in the absence of other processes contributing to their changes. To identify the formation site a well-designed hydrographic winter program is needed, which covers most parts of the West Greenland shelf with synoptic observations. The program should run long enough (several years) to observe dominant BBPW conditions two or three times.

The origin behind hydrographic changes such as GSAs are questioned by the presence of BBPW on the West Greenland coast at ~64°N. GSAs are presently described to be large salinity (temperature) anomalies propagating around the subpolar North Atlantic Ocean circulation system with timescales of 6–13 years and with arrival times at West Greenland in 1969–1970, 1982, and 1989–1990. The time series presented here reveal that the GSAs are unlikely to have been caused by advection of anomalies that travel along the large-scale circulation system, as illustrated by the presence of BBPW as far south on the West Greenland coast as ~64°N. More likely, they are shifts of water masses caused by changes in the production of BBPW and in the position and/or strength of oceanic currents. Therefore, we advocate for a new focus on temporal and spatial variations of the winter mode water mass, BBPW, and GSAs.

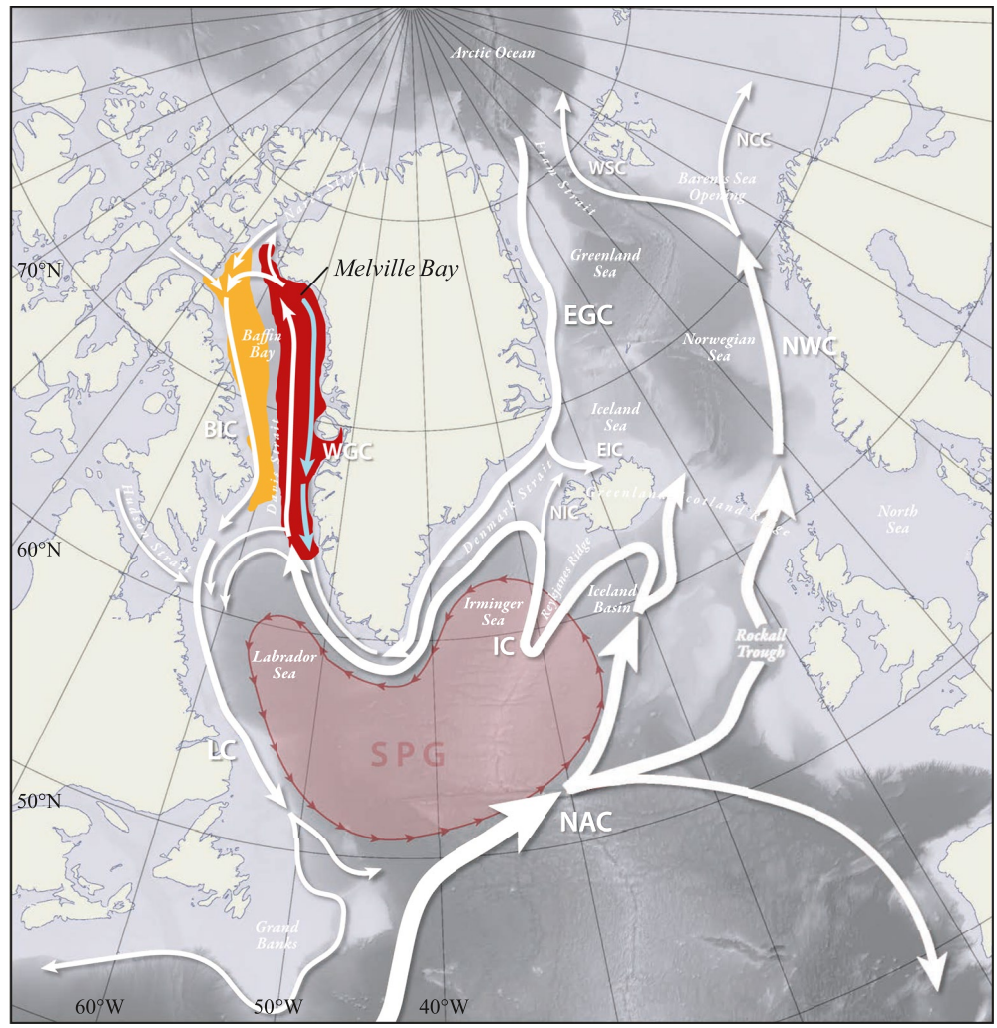

Figure 11. Schematic outline of the distribution of Baffin Bay Polar Water (BBPW) during years when BBPW reached as far south as Fyllas Banke at the West Greenland coast. Red is for the BBPW layer found close to the surface and yellow for the BBPW layer found at a deeper level. Also shown are a suggested upper layer currents in light blue in case the BBPW formation site is limited to the northeastern part of Baffin Bay. (The basis Figure is shown in Figure 1a above and adapted from Tesdal & Haine, 2020, Figure 1, JGR-Oceans).

Data Availability Statement

Data used are available from the International Council for the Exploration of the Sea (ICES, www.ices.dk). Monthly GF3 (2005–2018) data from the Greenland Ecosystem Monitoring Programme (GEM; www.g-e-m.dk) were provided by the Greenland Institute of Natural Resources, Nuuk, Greenland.

References

Addison, V. G., Jr. (1987). *Physical oceanography of the northern Baffin Bay-Nares strait region*. (M.Sc. Thesis). Naval Postgraduate School.

Bâcle, J., Carmack, E. C., & Ingram, R. G. (2002). Water column structure and circulation under the North Water during spring transition: April–July 1998. *Deep Sea Research II*, *49*, 4907–4925.

Belkin, I. M. (2004). Propagation of the "Great salinity anomaly" of the 1990s around the northern North Atlantic. *Geophysical Research Letters*, *31*, L08306. https://doi.org/10.1029/2003GL019334

Belkin, I. M., Levitus, S., Antonov, J., & Malmberg, S.-A. (1998). "Great salinity anomalies" in the north Atlantic. *Progress in Oceanography*, *41*, 1–68. https://doi.org/10.1016/s0079-6611(98)00015-9

Bendtsen, J., Rysgaard, S., Carlson, D. F., Meire, L., & Sejr, M. K. (2021). Vertical mixing in stratified fjords near tidewater outlet glaciers along Northwest Greenland. *Journal of Geophysical Research: Oceans*, *126*, e2020JC016898. https://doi.org/10.1029/2020JC016898

Bigg, G. R., & Wadley, M. R. (2007). Simulation of ''great salinity anomalies'' in coupled climate models. *Journal of Geophysical Research*, *112*, C03017. https://doi.org/10.1029/2006JC003475

Acknowledgments
Dedicated to Svend-Aage Malmberg and his three friends Jens Meincke, Bob Dickson and Johan Blindheim. This study received financial support from the Greenland Climate Research Centre and Greenland Research Council. L. M. was funded by the research program VENI with project 016.Veni.192.150 from the Dutch Research Council (NWO). S. R. was funded by NSERC in Canada and Aage V. Jensen Foundations. We would like to thank Flemming Heinrich, Lars Heilmann, Louise Mølgaard, Thomas Krogh, Else Ostermann, Bror, and many others for field assistance. Data used are available from the International Council for the Exploration of the Sea (ICES, www.ices.dk). Monthly GF3 (2005–2018) data from the Greenland Ecosystem Monitoring Programme (GEM; www.g-e-m.dk) were provided by the Greenland Institute of Natural Resources, Nuuk, Greenland. The Greenland Ecosystem Monitoring Programme is funded by the Danish Ministry of Climate, Energy and Utilities and Ministry of Environment of Denmark. We also would like to thank three anonymous reviewers for their detailed reviews that significantly improved the manuscript.

Bourke, R. H., Addison, V. G., & Paquette, R. G. (1989). Oceanography of Nares Strait and northern Bartin Bay in 1986 with emphasis on deep and bottom water formation. *Journal of Geophysical Research*, *94*(C6), 8289–8302. https://doi.org/10.1029/JC094iC06p08289

Buch, E., Pedersen, S. A., & Ribergaard, M. H. (2004). Ecosystem variability in West Greenland waters. *Journal of Northwest Atlantic Fishery Science*, *34*, 13–28. https://doi.org/10.2960/j.v34.m479

Burgers, T. M., Miller, L. A., Thomas, H., Else, B. G. T., Gosselin, M., & Papakyriakou, T. (2017). Surface water pCO_2 variations and sea-air CO_2 fluxes during summer in the Eastern Canadian Arctic. *Journal of Geophysical Research: Oceans*, *122*, 9663–9678. https://doi.org/10.1002/2017JC013250

Curry, B., Lee, C. M., & Petrie, B. (2011). Volume, freshwater, and heat fluxes through Davis Strait, 2004–05. *Journal of Physical Oceanography*, *41*, 429–436. https://doi.org/10.1175/2010jpo4536.1

Dickson, R. R., Meincke, J., Malmberg, S.-A., & Lee, A. J. (1988). The "great salinity anomaly" in the northern North Atlantic 1968–1982. *Progress in Oceanography*, *20*, 103–151. https://doi.org/10.1016/0079-6611(88)90049-3

Dooley, H. D., Martin, J. H. A., & Ellett, D. J. (1984). Abnormal hydrographic conditions in the Northeast Atlantic during the 1970s. Rapports et Procès-Verbaux des Réunions. *Conseil International pour lExploration de la Mer*, *185*, 179–187.

Ellett, D. J., & MacDougall, N. (1983). Some monitoring results from west of Britain. *IOC Technical Series Report*, *24*, 21–25.

Gladish, C. V., Holland, D. M., & Lee, C. M. (2015). Oceanic boundary conditions for Jakobshavn glacier. Part II: Provenance and sources of variability of Disko Bay and Ilulissat icefjord waters, 1990–2011. *Journal of Physical Oceanography*, *45*(1), 33–63. https://doi.org/10.1175/JPO-D-14-0045.1

Haak, H., Jungclaus, J., Mikolajewicz, U., & Latif, M. (2003). Formation and propagation of great salinity anomalies. *Geophysical Research Letters*, *30*, 1473. https://doi.org/10.1029/2003GL017065

Hátún, H., Lohmann, K., Matei, D., Jungclaus, J. H., Pacariz, S., Bersch, M., et al. (2016). An inflated subpolar gyre blows life toward the northeastern Atlantic. *Progress in Oceanography*, *147*, 49–66. https://doi.org/10.1016/j.pocean.2016.07.009

Holliday, N. P., Bersch, M., Berx, B., Chafik, L., Cunningham, S., Florindo-López, C., et al. (2020). Ocean circulation causes the largest freshening event for 120 years in eastern subpolar North Atlantic. *Nature Communications*, *11*, 585. https://doi.org/10.1038/s41467-020-14474-y

Juul-Pedersen, T., Arendt, K. E., Mortensen, J., Blicher, M. E., Søgaard, D. H., & Rysgaard, S. (2015). Seasonal and interannual phytoplankton production in a sub-Arctic tidewater outlet glacier fjord, SW Greenland. *Marine Ecology Progress Series*, *524*, 27–38. https://doi.org/10.3354/meps11174

Kenigson, J. S., & Timmermans, M.-L. (2021). Nordic seas hydrography in the Context of Arctic and North Atlantic ocean dynamics. *Journal of Physical Oceanography*, *51*, 101–114. https://doi.org/10.1175/JPO-D-20-0071.1

Khazendar, A., Fenty, I. G., Carroll1, D., Gardner, A., Lee, C. M., Fukumori, I., et al. (2019). Interruption of two decades of Jakobshavn Isbrae acceleration and thinning as regional ocean cools. *Nature Geoscience*, *12*, 277–283. https://doi.org/10.1038/s41561-019-0329-3

Kikuchi, T., Hatakeyama, K., & Morison, J. H. (2004). Distribution of convective lower Halocline water in the eastern Arctic Ocean. *Journal of Geophysical Research*, *109*, C12030. https://doi.org/10.1029/2003JC002223

Kim, W. M., Yeager, S., & Danabasoglu, G. (2021). Revisiting the causal connection between the great salinity anomaly of the 1970s and the Shutdown of Labrador Sea deep convection. *Journal of Climate*, *34*, 675–696. https://doi.org/10.1175/JCLI-D-20-0327.1

Lehmann, N., Kienast, M., Granger, J., & Tremblay, J.-É. (2022). Physical and biogeochemical influences on nutrients through the Canadian Arctic Archipelago: Insights from nitrate isotope ratios. *Journal of Geophysical Research: Oceans*, *127*, e2021JC018179. https://doi.org/10.1029/2021JC018179

Liang, Y., Bi, H., Wang, Y., Huang, H., Zhang, Z., Huang, J., & Liu, Y. (2021). Role of extratropical wintertime cyclones in regulating the variations of Baffin Bay sea ice export. *Journal of Geophysical Research: Atmospheres*, *126*, e2020JD033616. https://doi.org/10.1029/2020JD033616

Martin, J. H. A., Dooley, H. D., & Shearer, W. (1984). *Ideas on the origin and biological consequences of the 1970's salinity anomaly* (Vol. 18). ICES C.M. 1984/Gen. https://doi.org/10.1016/0301-0511(84)90108-x

McCartney, M. S., & Talley, L. D. (1982). The subpolar mode water of the North Atlantic Ocean. *Journal of Physical Oceanography*, *12*, 1169–1188. https://doi.org/10.1175/1520-0485(1982)012<1169:TSMWOT>2.0.CO;2

Melling, H., Gratton, Y., & Ingram, G. (2001). Ocean circulation within the north water polynya of Baffin Bay. *Atmosphere-Ocean*, *39*(3), 301–325. https://doi.org/10.1080/07055900.2001.9649683

Mortensen, J. (2015). *Report on hydrographic conditions off southwest Greenland June/July 2014*. (NAFO SCR Doc. 15/01). Serial No. N6416). Northwest Atlantic Fisheries Organizations.

Mortensen, J., Bendtsen, J., Lennert, K., & Rysgaard, S. (2014). Seasonal variability of the circulation system in a West Greenland tidewater outlet glacier fjord, Godthåbsfjord (64°N). *Journal of Geophysical Research: Earth Surface*, *119*, 2591–2603. https://doi.org/10.1002/2014JF003267

Mortensen, J., Bendtsen, J., Motyka, R. J., Lennert, K., Truffer, M., Fahnestock, M., & Rysgaard, S. (2013). On the seasonal freshwater stratification in the proximity of fast-flowing tidewater outlet glaciers in a sub-Arctic sill fjord. *Journal of Geophysical Research: Oceans*, *118*, 1382–1395. https://doi.org/10.1002/jgrc.20134

Mortensen, J., Lennert, K., Bendtsen, J., & Rysgaard, S. (2011). Heat sources for glacial melt in a subarctic fjord (Godthåbsfjord) in contact with Greenland Ice Sheet. *Journal of Geophysical Research*, *116*, C01013. https://doi.org/10.1029/2010JC006528

Mortensen, J., Rysgaard, S., Arendt, K. E., Juul-Pedersen, T., Søgaard, D. H., Bendtsen, J., et al. (2018). Local coastal water masses control heat levels in a west Greenland tidewater glacier fjord. *Journal of Geophysical Research: Oceans*, *123*, 8068–8083. https://doi.org/10.1029/2018JC014549

Mortensen, J., Rysgaard, S., Bendtsen, J., Lennert, K., Kanzow, T., Lund, H., & Meire, L. (2020). Subglacial discharge and its down-fjord transformation in West Greenland fjords with an ice mélange. *Journal of Geophysical Research: Oceans*, *125*, e2020JC016301. https://doi.org/10.1029/2020JC016301

Muench, R. D. (1970). *The physical Oceanography of the northern Baffin Bay region*. (Doctor of Philosophy). University of Washington.

Myers, P. G., Castro de la Guardia, L., Fu, C., Gillard, L. C., Grivault, N., Hu, X., et al. (2021). Extreme high Greenland blocking index leads to the reversal of Davis and Nares strait net transport towards the Arctic Ocean. *Geophysical Research Letters*, *48*, e2021GL094178. https://doi.org/10.1029/2021GL094178

Myers, P. G., Donnelly, C., & Ribergaard, M. H. (2009). Structure and variability of the West Greenland Current in summer derived from 6 repeated standard sections. *Progress in Oceanography*, *80*, 93–112. https://doi.org/10.1016/j.pocean.2008.12.003

Myers, P. G., & Ribergaard, M. H. (2013). Warming of the polar water layer in Disko Bay and potential impact on Jakobshavn Isbrae. *Journal of Physical Oceanography*, *43*, 2629–2640. https://doi.org/10.1175/JPO-D-12-051.1

Nansen, F. (1912). Das Bodenwasser und die abkühlung des meres. *Internationale Revue der Gesamten Hydrobiologie und Hydrographie*, *1*(1), 1–42.

Padman, L., Siegfried, M. R., & Fricker, H. A. (2018). Ocean tide influences on the Antarctic and Greenland ice sheets. *Reviews of Geophysics*, *56*, 142–184. https://doi.org/10.1002/2016RG000546

Randelhoff, A., Oziel, L., Massicotte, P., Bécu, G., Galí, M., Lacouret, L., et al. (2019). The evolution of light and vertical mixing across a phytoplankton ice-edge bloom. *Elementa Science of the Anthropocene*, *7*, 20. https://doi.org/10.1525/elementa.357

Ribergaard, M. H., Pedersen, S. A., Ådlandsvik, B., & Kliem, N. (2004). Modelling the ocean circulation on the West Greenland shelf with special emphasis on northern shrimp recruitment. *Continental Shelf Research*, *24*, 1505–1519.

Richter, A., Rysgaard, S., Dietrich, R., Mortensen, J., & Petersen, D. (2011). Coastal tides in West Greenland derived from tide gauge records. *Ocean Dynamics*, *61*, 39–49. https://doi.org/10.1007/s10236-010-0341-z

Rysgaard, S., Boone, W., Carlson, D., Sejr, M. K., Bendtsen, J., Juul-Pedersen, T., et al. (2020). An updated view on water masses on the pan-west Greenland continental shelf and their link to proglacial fjords. *Journal of Geophysical Research: Oceans*, *125*, e2019JC015564. https://doi.org/10.1029/2019JC015564

Stuart-Lee, A. E., Mortensen, J., van der Kaaden, A.-S., & Meire, L. (2021). Seasonal hydrography of Ameralik: A southwest Greenland fjord impacted by a land-terminating glacier. *Journal of Geophysical Research: Oceans*, *126*, e2021JC017552. https://doi.org/10.1029/2021JC017552

Tesdal, J.-E., & Haine, T. W. N. (2020). Dominant terms in the freshwater and heat budgets of the subpolar North Atlantic Ocean and Nordic seas from 1992 to 2015. *Journal of Geophysical Research: Oceans*, *125*, e2020JC016435. https://doi.org/10.1029/2020JC016435

Wadley, M. R., & Bigg, G. R. (2004). "Great Salinity Anomalies" in a coupled climate model. *Geophysical Research Letters*, *31*, L18302. https://doi.org/10.1029/2004GL020426

Wadley, M. R., & Bigg, G. R. (2006). Are "great salinity anomalies" advective? *Journal of Climate*, *19*, 1080–1088.

Wüst, G. (1928). *Der urspung der Atlantischen Tiefenwässer* (pp. 506–534). Zeitschr. Gefellsch. F. Erdkde.